Directional Wave Information From the SeaSonde

Belinda Lipa and Bruce Nyden

***Abstract*—This paper describes methods used for the derivation of wave information from SeaSonde data, and gives examples of their application to measured data. The SeaSonde is a compact high-frequency (HF) radar system operated from the coast or offshore platform to produce current velocity maps and local estimates of the directional wave spectrum. Two methods are described to obtain wave information from the second-order radar spectrum: integral inversion and fitting with a model of the ocean wave spectrum. We describe results from both standard- and long-range systems and include comparisons with simultaneous measurements from an S4 current meter. Due to general properties of the radar spectrum common to all HF radar systems, existing interpretation methods fail when the waveheight exceeds a limiting value defined by the radar frequency. As a result, standard- and long-range SeaSondes provide wave information for different wave height conditions because of their differing radar frequencies. Standard-range SeaSondes are useful for low and moderate waveheights, whereas long-range systems with lower transmit frequencies provide information when the waves are high. We propose a low-cost low-power system, to be used exclusively for local wave measurements, which would be capable of switching transmit frequency when the waveheight exceeds the critical limit, thereby allowing observation of waves throughout the waveheight range.**

***Index Terms*—High-frequency (HF) radar oceanography, remote sensing, wave measurements.**

I. Introduction

THE potential of HF radar devices for the remote measurement of sea-surface parameters has been recognized since Crombie [1] observed and identified the distinctive features of sea-echo Doppler spectra. Barrick [2], [3] derived the exact theoretical formulation that expresses the HF sea-echo Doppler spectrum in terms of the ocean waveheight directional spectrum and the surface current velocity. Since then, methods have been developed to interpret the sea echo spectrum in terms of these theoretical relationships. Commercial systems, which have been available for several years, use these methods to produce current maps and directional wave information.

The first HF radar systems to be developed were phased arrays, which ideally have narrow radar beams, followed by smaller systems with multiple broad beams. Although the interpretation of "narrow-beam" signals backscattered from the sea is simpler, the disadvantage of phased-array systems for most applications is their large physical size and consequent difficult installation procedures and high operating cost. It is mainly for this reason that compact, transportable systems were developed in the seventies, followed by the SeaSonde, which has been available commercially since 1990. The SeaSonde has three small antennas, two crossed loops and a monopole. Interpretation of the signal voltages using Barrick's equations yields both the surface current field and directional ocean wave parameters.

Methods to derive the directional wave spectrum from a narrow beam radar were developed by Lipa and Barrick in the seventies and considerably extended by Wyatt [4]–[7], Wyatt and Ledgard [8], Howell and Walsh [9], Hisaki [10], Hashimoto *et al.* [11]. This paper describes the extension of the narrow-beam methods described by Lipa and Barrick [12] to apply to broad-beam SeaSonde data.

The SeaSonde provides robust measurements of ocean surface currents, which are obtained from the dominant first-order peaks in the radar echo spectrum. However the derivation of wave information from the second-order radar spectrum is more fragile, partly because the lower-energy second-order spectrum is closer to the noise floor, and more likely to be contaminated. In addition, for the high wave conditions of greatest interest, the radar spectrum saturates when the waveheight exceeds a limit defined by the radar transmit frequency. Above this waveheight limit, the radar spectrum loses its definitive shape and the perturbation expansions on which Barrick's equations are based fail to converge. At present such radar spectra are not amenable to analysis. This saturation effect is common to all HF radar systems.

When the radar spectrum saturates, first-order echo merges with second- and third-order, and its interpretation is not possible using existing methods. This broadening of the Doppler spectrum was demonstrated for example by Wyatt [7]. When normal interpretation methods are applied to saturated spectra, waveheight can be underestimated, as noted by Lipa and Barrick [12] and predicted theoretically by Hisaki [13]. The saturation limit on the significant waveheight is defined approximately by

$$h_{\mathrm{sat}} = \frac{2}{k_0} \tag{1}$$

where k_0 is the radar wavenumber. For a standard-range SeaSonde (transmit frequency 13 MHz), the value of h_{sat} is 7.4 m; this value increases to 20 m for a long-range SeaSonde (transmit frequency 4–5 MHz). Hence, the observation of extremely high waves with a SeaSonde requires the use of the long-range system.

In this paper, we describe two methods for use with SeaSonde systems, the first, integral inversion, provides detailed wave information under a somewhat restricted set of conditions. The second involves fitting a model of the ocean wave spectrum

Manuscript received October 8, 2003; accepted October 7, 2004. This work was supported in part by funding from the National Science Foundation, the Sonoma County Water Agency, and the Office of Research, University of California-Davis. Contribution #2204 from Bodega Marine Laboratory, University of California-Davis. Associate Editor: L. Wyatt.

B. J. Lipa is with Codar Ocean Sensors, Portola Valley, CA 94028 USA (e-mail: blipa@codaros.com).

B. B. Nyden is with Codar Ocean Sensors, Los Altos, CA 94024 USA. He is also with the Bodega Marine Laboratory, Bodega Bay, CA 94923 USA (e-mail: bruce@codaros.com).

Digital Object Identifier 10.1109/JOE.2004.839929

to the radar data to give estimates of waveheight, centroid period, and direction. Operational software for both standard- and long-range SeaSondes is based on the second method, as it can be applied under a wide range of conditions.

Section II gives the basis of radar spectral theory used in the paper. Section III discusses features of SeaSonde cross spectra. Section IV describes models for the ocean wave directional spectrum used in the analysis. Section V describes methods used to interpret the radar cross spectra. Section VI describes effects of varying the radar transmit frequency. Section VII describes application to measured data from both standard- and long-range SeaSondes at several locations. Results from a standard-range SeaSonde located at Bodega Marine Laboratory are compared with simultaneous measurements made by an S4 current meter. Examples are given of wave results obtained from long-range Seasondes located at Nojima and Hachijo, Japan during periods of high waveheight. Finally we illustrate the complementary nature of wave measurements from standard- and long-range SeaSondes using results from neighboring systems on the Oregon coast.

II. Radar Spectral Theory

We assume herein that the waves producing the second-order scatter do not interact with the ocean floor. This requires that the water depth over most of the radar range ring obeys the condition

$$\frac{2\pi d}{L} > 0.8 \tag{2}$$

where d is the water depth and L is the dominant ocean wavelength.

Barrick [2] showed that the narrow-beam first-order radar cross section at frequency ω and direction φ is defined in terms of the ocean wave spectrum at the Bragg wavenumber by

$$\sigma^1(\omega,\varphi) = k_0^4 \sum_{m'=\pm 1} S\left(2k_0, \varphi + (m'+1)\frac{\pi}{2}\right)\delta(\omega - m'\omega_B) \tag{3}$$

where $S(k,\varphi)$ is the directional ocean wave spectrum for wavenumber k and direction φ and ω_B is the Bragg frequency given by $\sqrt{2gk_0}$, where g is the gravitational constant.

Barrick [3] gives the narrow-beam second-order radar cross section as

$$\sigma^2(\omega,\varphi) = k_0^4 \sum_{m,m'=\pm 1} \int_0^{2\pi}\int_{-\infty}^{\infty} |\Gamma^2| S(k,\theta+\varphi+m\pi) \cdot S(k',\theta+\varphi+m'\pi)\delta(\omega - m\sqrt{gk} - m'\sqrt{gk'})kdkd\theta \tag{4}$$

where Γ is the radar coupling coefficient, which is the incoherent sum of hydrodynamic and electromagnetic terms and k, k' are the wavenumbers of the two scattering ocean waves. The values of m and m' in (4) define the four possible combinations of direction of the two scattering waves and also the four sidebands that surround the first-order peaks, see Lipa and Barrick, [12]. The two ocean scattering wave vectors $\tilde{k}$, $\tilde{k}'$ obey the constraint

$$\tilde{k} + \tilde{k}' = -2\tilde{k}_0 \tag{5}$$

where $\tilde{k}_0$ is the radar wave vector.

Lipa and Barrick [14] describe the extension of the theory to apply to a broad-beam system such as the SeaSonde, assuming ideal antenna patterns. From the antenna voltage cross spectra, we form as intermediate data products the first five Fourier angular coefficients of the broad-beam return over a selected range ring surrounding the radar. These coefficients, $b_n^{1,2}(\omega)$ are defined in terms of the narrow-beam first and second-order return through

$$b_n^{1,2}(\omega) = \int_{\gamma_1}^{\gamma_2} \sigma^{1,2}(\omega,\varphi) tf_n(\varphi) d\varphi \tag{6}$$

where the integration is performed over angle around the radar range cell between the coastline angles defined by γ_1, γ_2 and the superscripts refer to first- and second-order, respectively. Here the five Fourier coefficients are designated by the index $n = -2, -1, 0, 1, 2$ and following the notation of Lipa and Barrick [14] the trigonometric functions $tf_n(\varphi)$ are given by

$$\begin{aligned} tf_n(\varphi) &= \sin(n\varphi) n < 0 \\ &= \cos(n\varphi) n \le 0. \end{aligned} \tag{7}$$

We plan to extend this theory to apply to measured antenna patterns in the future.

III. SeaSonde Sea-Echo Cross Spectra

Lipa and Barrick [15] describe how the voltage time series from the separate SeaSonde antenna elements are Fourier transformed to give complex voltage spectra and their self- and cross-spectra, which can be interpreted using Barrick's theoretical formulation. Fig. 1 shows two examples of self-spectra from the three SeaSonde antennas, measured when the waveheight is above and below the saturation limit $h_{\rm sat}$ defined by (1).

The spectra in Fig. 1(a) were measured when the waveheight was less than $h_{\rm sat}$. The form of the spectrum is similar to that of a narrow-beam sea-echo spectrum, but is spread by the interaction of the broad beams with the varying surface current field. The dominant spectral peaks are produced by scatter from the first-order Bragg waves of wavelength one-half the radar transmit frequency moving directly toward or away from the radar. With an infinitely narrow beam, the first-order peak would be an impulse function in frequency, shifted from the ideal Bragg position by an amount proportional to the radial component of the current velocity. For broad beam sea echo, there is a different Doppler shift for each angle of return, causing the beam to be spread out in frequency. The first-order peaks are typically two orders of magnitude higher than the surrounding continuum, from which they are separated by well-defined nulls. The continuum arises from higher-order scatter, the greater part of which arises from scatter from pairs of ocean waves. Ocean wave information is obtained from interpretation of this higher order spectrum, normalized by the first-order energy.

The spectra in Fig. 1(b) were measured when the waveheight is greater than $h_{\rm sat}$.The first- and higher-order spectral regions are merged together. Such spectra cannot at present be interpreted successfully for either waves or current velocity information, as they cannot be separated into first- and second-order regions.

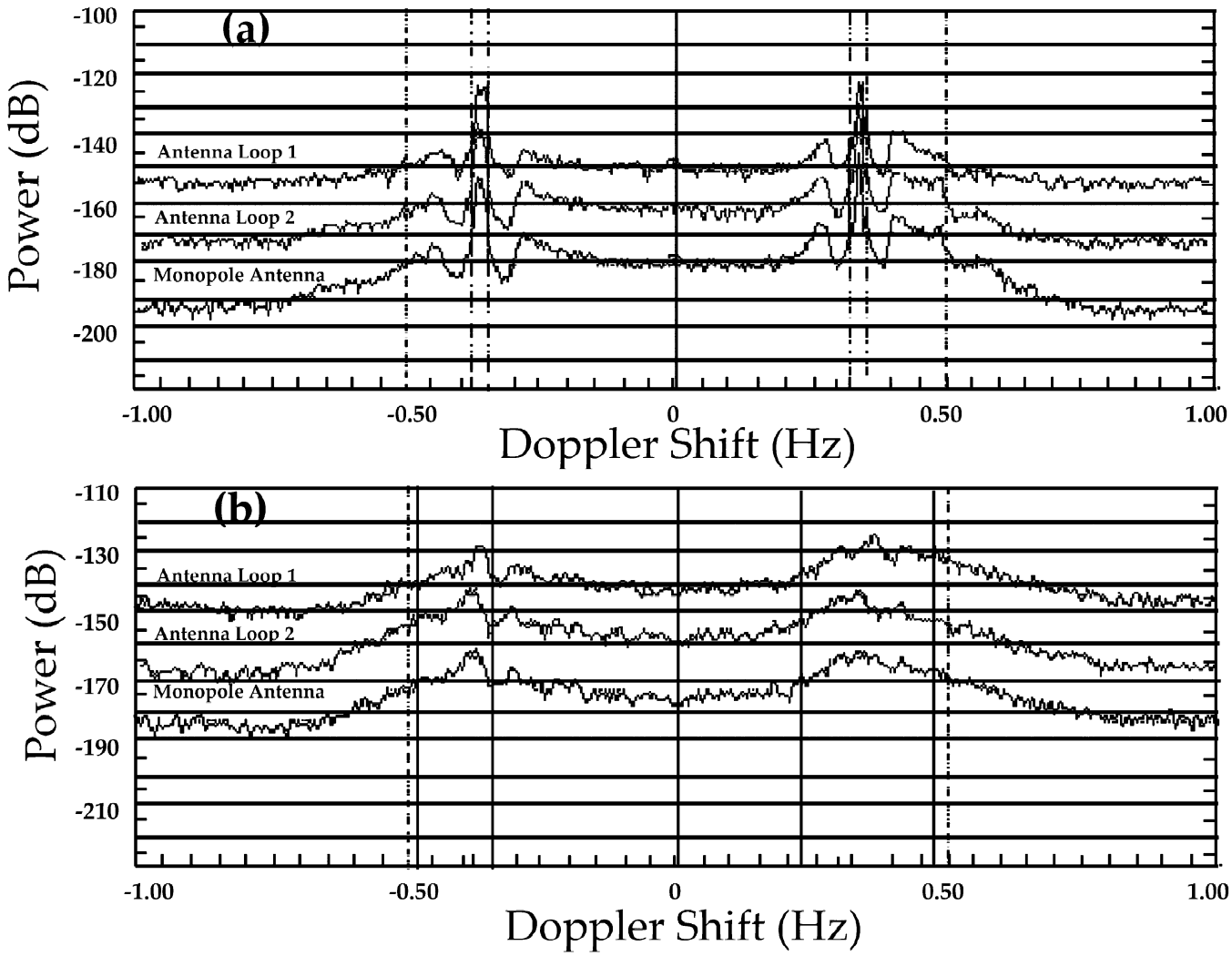

Fig. 1. Example of self-spectra, averaged over ten minutes. As labeled, the upper two curves are from the loop antennas, the lower curve from the monopole antenna: the curves are displaced vertically by 20 dB to allow ease of viewing. The vertical lines surrounding the Bragg peaks indicate the boundaries selected by the software to separate the first- and second-order structure. (a) Spectra measured by the standard-range SeaSonde at Bodega Marine Lab. at 4 A.M. November 30, 2001, when the waveheight was below the saturation limit. (b) Saturated spectra obtained by the Washburn standard-range SeaSonde at 8 P.M. December 14, 2001, when the waveheight exceeds the saturation limit.

IV. Ocean Wave Directional Spectral Models

A. Assumptions

We assume that the ocean wave spectrum is homogeneous over the radar range cell used for the analysis. Because of this assumption, the smaller close-in radar range cells are used for wave analysis.

Close to shore, there is insufficient fetch to generate long-period waves. When operating from shore, the assumption was made that waves of period larger than 6 s arrive from a 180° sector defining the open ocean. For shorter waves and when operating from a platform or island, no restriction was placed on wave direction.

We consider only deep water conditions and ignore wave refraction.

B. Ocean Wave Spectral Models

To estimate the directional ocean wave spectrum, we use two model ocean wave spectra $S(k,\varphi)$.

1) General Fourier Series: This model defines the ocean spectrum as the sum of the first five terms of a Fourier series over direction:

$$S(k,\varphi) = \sum_{n=-2}^{2} c_n(k) t f_n(\varphi). \tag{8}$$

The Fourier angular coefficients $c_n(k)$ are independent real functions and provide similar information to that given by a pitch-and-roll wave buoy.

When the radar operates from shore, $S(k,\varphi)$ is set to zero for offshore waves of period greater than 6 s, as discussed in Section IV-A.

2) Pierson-Moskowitz Model With Cardioid Directional Distribution: The second model for the ocean spectrum is defined as the product of directional and nondirectional factors

$$S(k,\varphi) = Z(k)\cos^4\left(\frac{\varphi-\varphi^*}{2}\right). \tag{9}$$

The directional factor in (9) has a cardioid distribution around the direction φ^*. For the nondirectional spectrum we

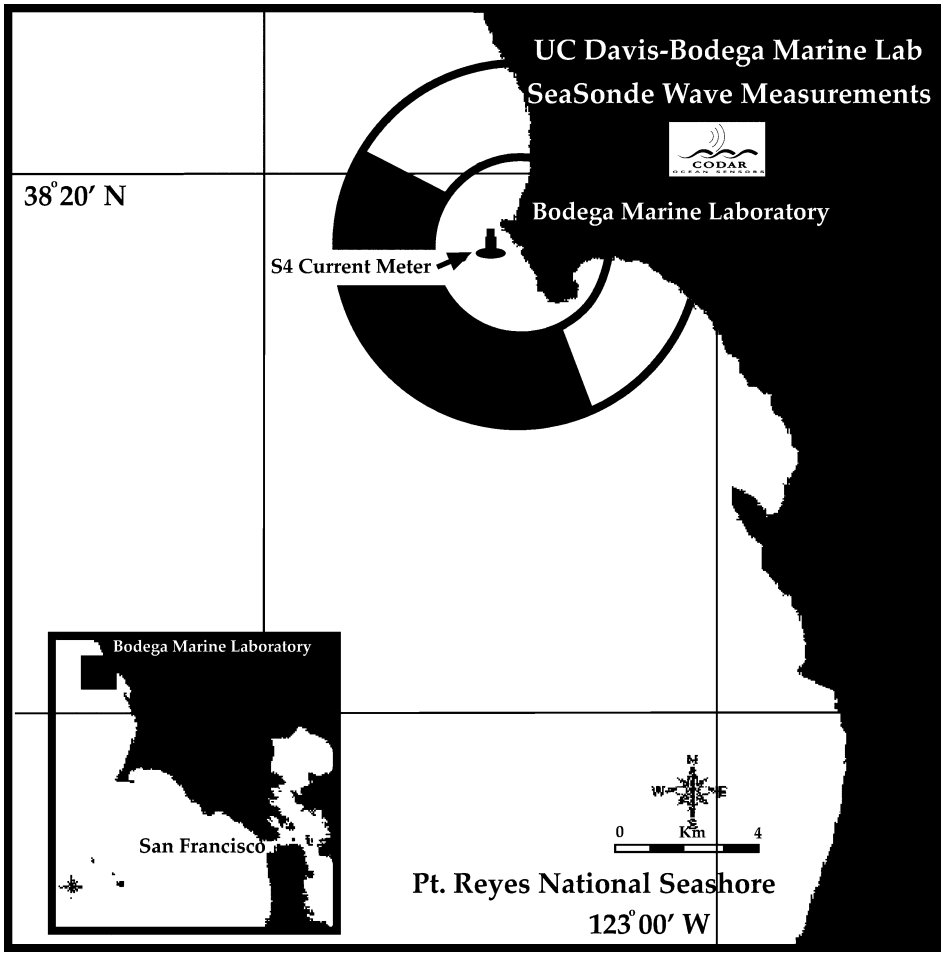

Fig. 2. The locations of the BML SeaSonde and the S4 current meter. The inset map shows the location on the California coast. Radar sea-echo from the second range cell is analyzed to give wave information. Radar coverage in the range cell is restricted by obstructing land to the shaded area shown.

use a Pierson-Moskowitz model. When the radar operates from shore, $S(k,\varphi)$ is set to zero for offshore waves of period greater than 6 s, as described in Section IV-A. The nondirectional factor $Z(k)$ is given by

$$Z(k) = \frac{Ae^{-0.74(k_c/k)^2}}{k^4} \tag{10}$$

with parameters k_c and a multiplicative constant A. The wave-height, centroid period and direction can be defined in terms of the model parameters. The significant waveheight follows from the directional spectrum through

$$h = 4\left(\int_0^\infty \int_{\gamma_1}^{\gamma_2} S(k,\varphi)dkd\varphi\right)^{1/2}. \tag{11}$$

V. Interpretation of the Radar Fourier Spectral Coefficients

There are three steps in the interpretation of the radar spectrum to give wave information. To start with, the first- and second-order regions are separated. Then, the first order region is analyzed to give the ocean wave spectrum at the Bragg wavenumber. Finally, the second-order radar spectrum is analyzed to give parameters of the total ocean wave spectrum. In the final step, the second-order spectrum is effectively normalized by the first-order, eliminating unknown multiplicative factors produced by antenna gains, path losses, etc.

To interpret the second-order spectrum, we used two approaches: the first is integral inversion to derive the Fourier coefficients of the general model described in Section IV-B-1. This method can be applied to standard-range SeaSonde data when the radar spectral energy for at least two second-order sidebands is above the noise floor. However, the approximations inherent in this approach are not valid for the long-range systems, due to their low transmit frequency. The second method is based on least-squares fitting of the radar spectrum with the model ocean wave spectrum described in Section IV-B-2. SeaSonde operational wave software is based on this method, and gives routine estimates of waveheight, period, and direction for both standard- and long-range systems under a wide range of conditions.

A. Separation of the First- and Second-Order Regions

SeaSonde software automatically searches for the nulls between the first- and second-order spectra and determines the Doppler frequencies and radar spectral data corresponding to the two regions.

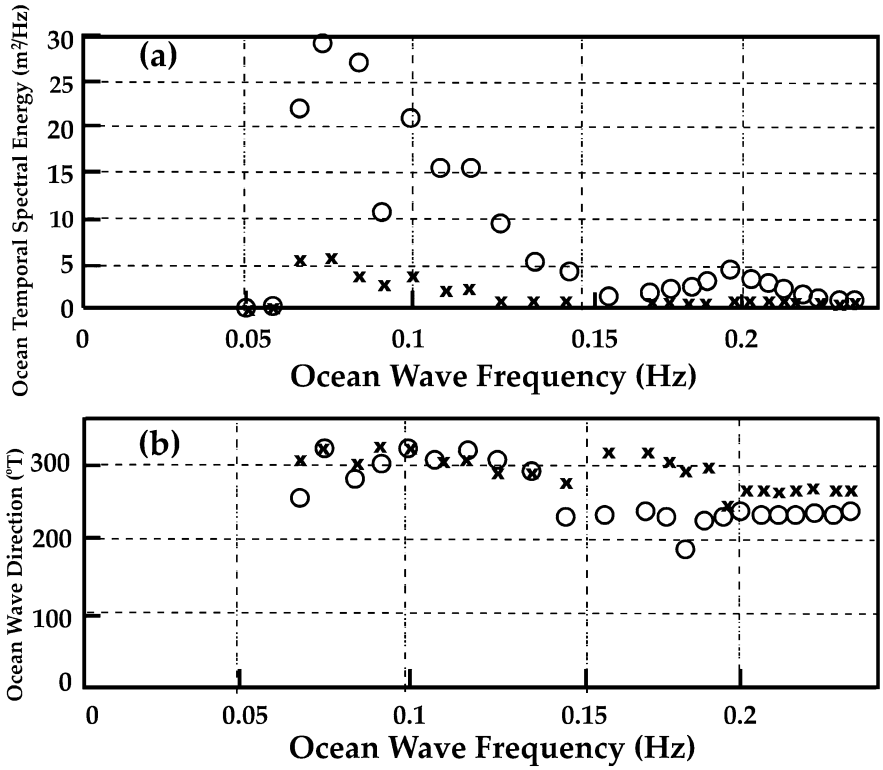

Fig. 3. Examples of wave information produced by integral inversion of the normalized second-order spectrum from the BML SeaSonde at 7 P.M. December 2, 2001 (circles) and 8 P.M. December 4, 2001 (crosses). (a) Ocean wave temporal spectrum versus wave frequency. (b) Ocean wave direction versus wave frequency.

B. Derivation of the Ocean Spectrum at the Bragg Wavenumber

The ocean wave directional spectrum at the Bragg wavenumber is obtained from the first-order spectral peaks. Inserting (3) for the narrow-beam radar cross section into (6) for the broad-beam coefficients gives the following equation for the pth first-order radar coefficient at a Doppler shift of magnitude ω, with positive, negative Doppler regions specified by values of m' equal to $+1$, -1, respectively.

$$b_p^1(m',\omega) = k_0^4 \cdot \int_{\gamma_1}^{\gamma_2} \delta(\omega - m'\omega_B) S \cdot \left(2k_0, \varphi + (m'+1)\frac{\pi}{2}\right) t f_p(\varphi) d\varphi. \quad (12)$$

Integrating over frequency over the first-order region gives

$$B_p^1(m') = \int b_p^1(m',\omega) d\omega = k_0^4 \int_{\gamma_1}^{\gamma_2} S\left(2k_0, \varphi + (m'+1)\frac{\pi}{2}\right) t f_p(\varphi) d\varphi. \quad (13)$$

Equation (13) defines a matrix equation for the integrated radar coefficients in terms of the ocean wave spectrum at the Bragg wavenumber. We then substitute the model ocean spectral model defined by (8) into (13), and derive the coefficients $c_n(k)$ by matrix inversion. As the Bragg waves are relatively short, we assume that they follow the wind, and an estimate of wind direction follows from the directional distribution defined by the derived Fourier coefficients. The derived nondirectional coefficient contains, in addition to the nondirectional spectral amplitude, unknown signal multiplicative factors.

C. Derivation of the Complete Ocean Wave Spectrum

To express the second-order SeaSonde data in terms of the directional spectrum, we insert (4) for the narrow-beam second-order radar cross section into (6) for the radar Fourier coefficients. This gives for the pth second-order radar coefficient for the radar sideband defined by m, m'

$$b_p^2(m,m',\omega) = k_0^4 \int_{\gamma}^{\gamma} \int_0^{2\pi} |\Gamma|^2 S(k, \theta + \varphi + m\pi) \cdot S(k', \theta + \varphi + m') \delta\left(\omega - mgk - m'\sqrt{gk'}\right) k dk d\theta d\varphi. \quad (14)$$

The right-hand side (RHS) of (14) is an integral over a product of spectral factors for the two scattering ocean waves and the radar coupling coefficient. To linearize this equation, we note that, as discussed by Lipa and Barrick [12], for frequencies close to the Bragg line, the wave vector of the shorter scattering ocean wave approximates the Bragg wave vector. The corresponding directional spectral factor is therefore approximately equal to that of the Bragg wave, which has been obtained from the first-order region. However, a better approximation is obtained by including the wavenumber variation along the constant Doppler frequency contour, assuming the Phillips equilibrium spectrum as follows:

$$S(k',\alpha) = S(2k_0,\alpha)\left(\frac{k_0}{k}\right)^4. \quad (15)$$

Substitution of (15) into (14) linearizes the integral equation for the radar coefficients in terms of the remaining spectral factor. As the spectral factor $S(2k_0,\alpha)$ is derived from the

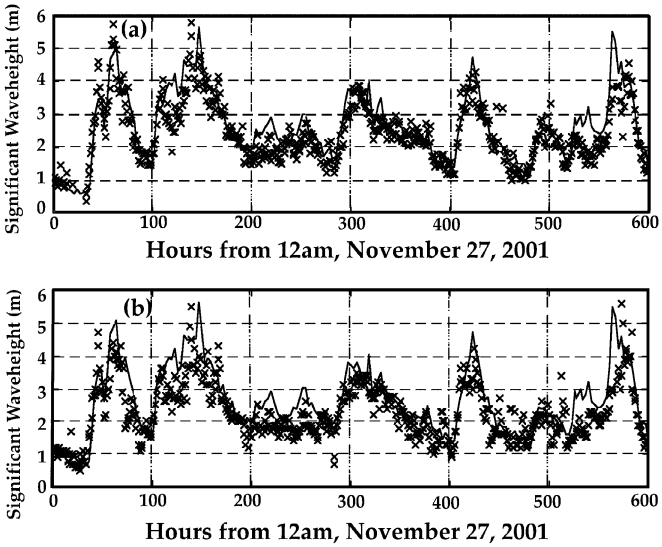

Fig. 4. Significant waveheight comparison at BML: The crosses are SeaSonde measurements, the continuous line is from the S4 current meter. (a) SeaSonde results obtained using model-fitting (b) SeaSonde results obtained using integral inversion.

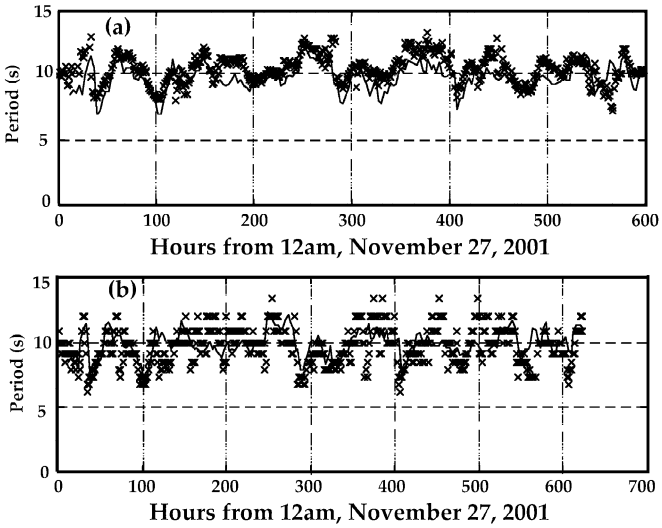

Fig. 5. Wave period comparison at BML. SeaSonde measurements of the period at the centroid of the spectrum (crosses) and from the S4 meter (continuous line). (a) SeaSonde results obtained using model-fitting. (b) SeaSonde results obtained using integral inversion.

first-order region, this step eliminates all unknown multiplicative factors such as antenna voltage drifts; therefore the system is self-calibrating for waveheight determination.

We then apply one of the following methods to interpret the linearized integral equation.

1) Integral Inversion: This method is based on Fourier series expansion of the ocean wave spectral model described in Section IV-B-I. Substituting the Fourier series defined by (8) into the linearized (14) reduces it to a matrix equation for the radar coefficients in terms of the ocean wave directional coefficients. Unfortunately the transformation matrix is typically too ill-conditioned to allow the latter to be determined by simple matrix inversion. We therefore simplify the equation using an approximation described by Lipa and Barrick [12]. As the frequency contours defined by a constant Doppler frequency on the RHS of (14) are approximately circular close to the Bragg

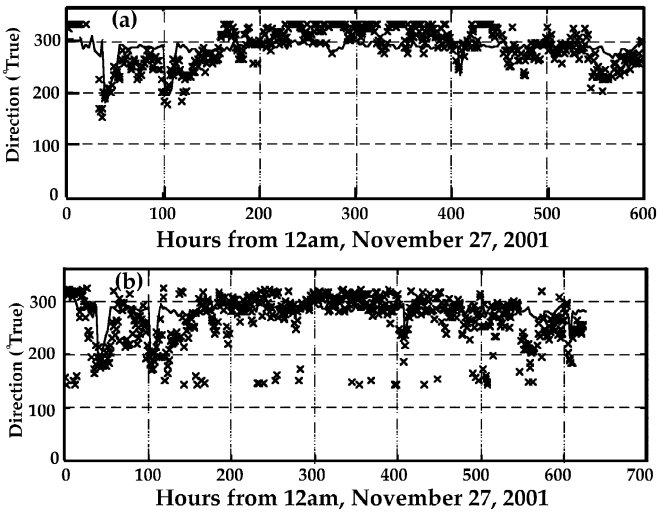

Fig. 6. Wave direction comparison at BML: SeaSonde measurements (crosses) and from the S4 meter (continuous lines). (a) SeaSonde results obtained using model-fitting. The analysis assumes that waves of period greater than 6 s are onshore, as discussed in Section IV-A. (b) SeaSonde results obtained using integral inversion.

TABLE I

	Standard Deviation	Bias	Correlation Coefficient
Model Fit			
Waveheight	0.65 m	-0.26 m	0.82
Wave period	1.7 s	0.8 s	0.43
Wave direction	36°	16°	0.47
Integral Inversion			
Waveheight	0.70 m	-0.38 m	0.81
Wave period	1.3 s	-0.18 s	0.52
Wave direction	42°	-6°	0.37

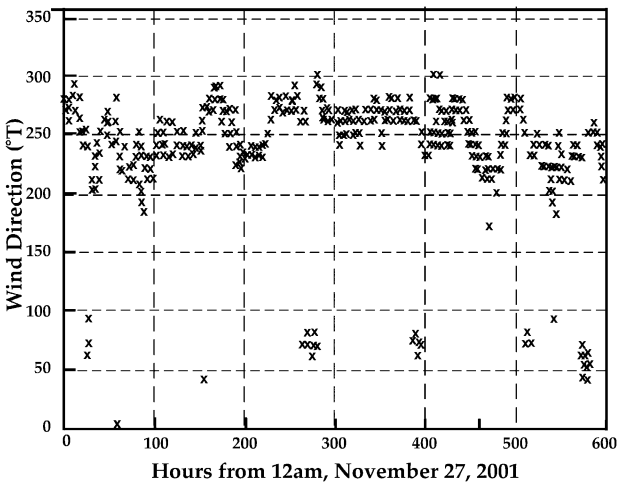

Fig. 7. Wind direction from the BML SeaSonde, calculated from the first-order radar cross spectra using the method described in Section V-B.

frequency, a given Doppler shift corresponds to a narrow band of ocean wavenumbers. Therefore in this region, we can represent the wavenumber band by its central value. For wave periods less than 6 s we also include a wavenumber variation along the constant Doppler frequency contour, as described by (15). These approximations result in a considerable simplification of the matrix equation, and the resulting transformation matrix is

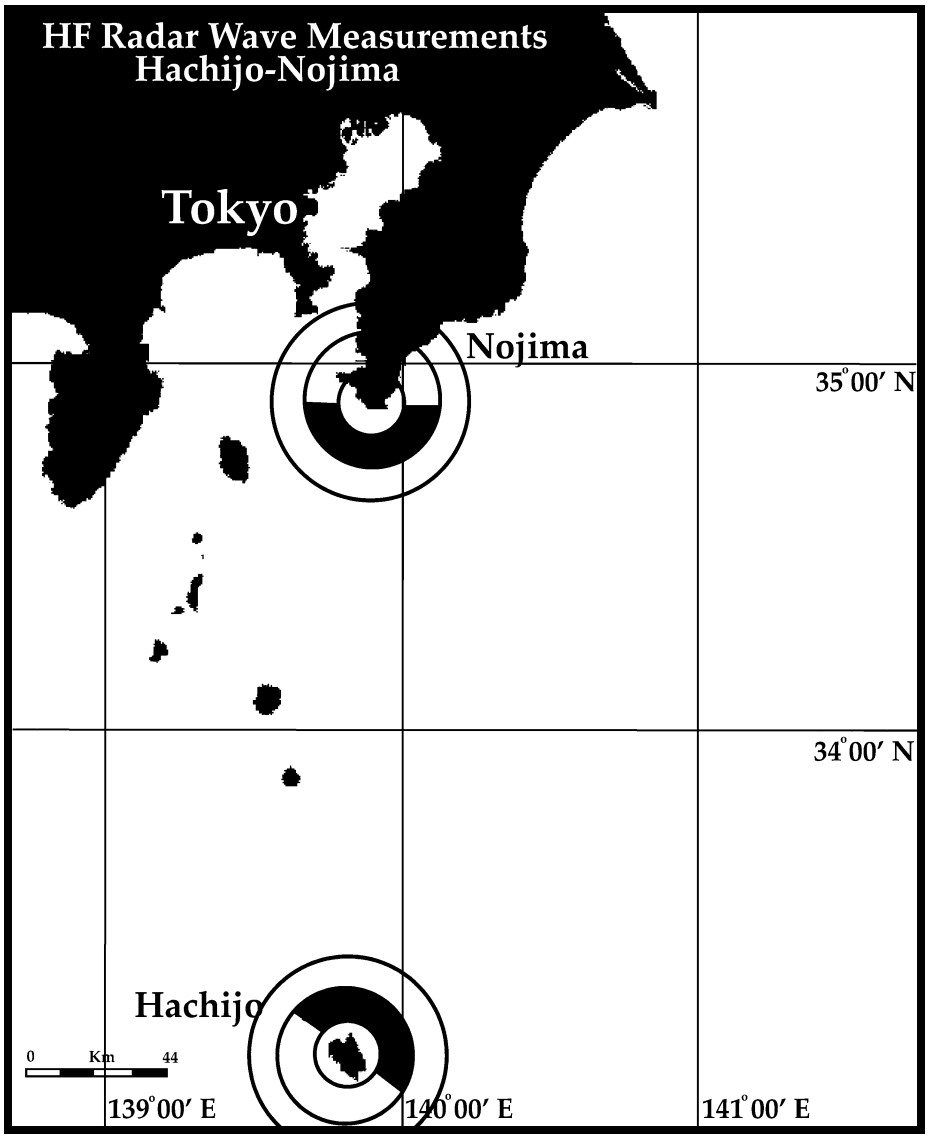

Fig. 8. The location of the long-range SeaSondes at Hachijo and Nojima, Japan. Radar sea-echo from the second range cell is analyzed to give wave information. Radar coverage in the range cell is restricted by obstructing land to the shaded area shown.

sufficiently well conditioned to allow the Fourier directional coefficients to be derived as a function of wavenumber.

Integral inversion provides the most detailed information on the directional ocean wave spectrum. The approximations used are adequate for standard-range Seasondes with radar transmit frequency above 12 MHz, but are inadequate for the long-range systems with transmit frequency below 5 MHz. In addition, at a given value of ocean wave frequency, successful matrix inversion requires that at the corresponding frequencies in the radar spectrum, at least two of the radar sidebands must be above the noise level for all three antennas. Noise in the radar spectrum may result in missing points in the derived ocean wave spectrum, leading to a low estimate for waveheight.

2) Model Fit: The Pierson-Moskowitz model for the ocean wave spectrum defined by (9) and (10) is substituted into the linearized (14). Second-order data is collected from the four second-order sidebands of hourly averaged cross spectra. Least-squares fitting to the radar Fourier coefficients is used to derive estimates of the significant wave height, centroid period, and direction. The SeaSonde operational software is based on this method, because of its wide applicability. An advantage of this method is that it uses all available data above the noise, including cases where only one sideband is usable.

VI. Effects of Radar Transmit Frequency

Increasing the radar transmit frequency has the following effects.

1) The second-order radar order spectrum increases relative to the noise.
2) The frequency width of the first-order spectrum increases in the presence of radial current shear, and may cover the second-order spectrum close to the first-order region when the current speed is high.
3) The saturation limit on waveheight decreases, meaning that information is not provided for the high waves that are often of greatest interest.

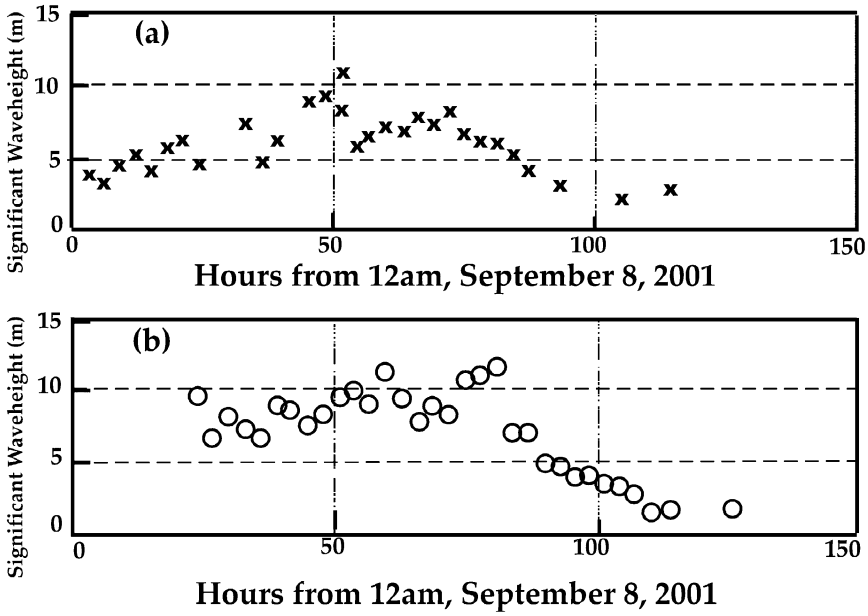

Fig. 9. Significant waveheight measured with long-range SeaSondes located at Hachijo and Noji during a storm, September 2001. (a) Hachijo. (b) Nojima.

As a result of these effects, standard range (13 MHz) SeaSondes are most effective in regions where the current velocities and wave velocities are not excessive. In practice, they produce wave information reliably except when the waveheight exceeds 7 m or the current velocity exceeds 4 m/s.

In contrast, long-range SeaSondes produce wave information only for high waves. Due to their low transmit frequencies, the second-order structure often falls below the noise floor. It is only for high waves that the second-order structure emerges from the noise, allowing the extraction of wave information. However, long-range systems do not have problems with radar spectral saturation or the spreading of the first-order line over the neighboring second-order structure.

VII. Application to Data

In this section, we give examples of wave results from SeaSondes at three locations.

Angles are measured clockwise from true north, and are defined as the direction the waves/wind are coming from. The upper (lower) period limit on derived wave spectra was set at 17 s (4 s), respectively.

A. Bodega Marine Laboratory (BML)

The locations of the SeaSonde and the S4 current meter at Bodega Marine Laboratory (BML) are shown in Fig. 2. We used the second radar range cell (shown shaded) in our calculations, which is 4 km from the site.

The transmit frequency of the BML Seasonde is approximately 13 MHz. In this region, the cross spectra rarely saturate at this radar frequency and current speeds are below 200 cm/s, so spreading of the first-order region over the second-order structure does not occur. Also there is low noise and little radar interference. Thus BML provides an ideal situation for the application of integral inversion techniques to give the directional ocean wave spectrum. Fig. 3 shows examples of results obtained using this method.

An InterOcean S4 electromagnetic current meter equipped with a pressure transducer was used to validate SeaSonde wave measurements at BML. The S4 was deployed on the sea floor approximately 1.2 km northwest of the SeaSonde's receive antenna at the outer edge of the first range cell. The current meter was deployed by divers and mounted to a rigid titanium pole in 32 m of water. The pole was extended approximately 2 m above the rocky bottom putting the S4's pressure sensor at a depth of approximately 30 m below mean sea level.

Continuous (2 Hz) pressure readings were made for 15-min periods every 3 h for approximately 6 wk from November 27 to December 21, 2001.

Estimates of wave heights and wave direction were derived from the water pressure data using InterOcean's proprietary wave software "WAVE for Windows" (WAVEWIN). The frequency cutoffs for processing were set at 0.0333 Hz for the lower frequency 0.177 Hz for the upper frequency based on the sensor's depth.

Figs. 4–6 show the significant waveheight, centroid period, wave and wind direction, over the 25-d period together with simultaneous S4 current meter measurements obtained by model fitting and integral inversion. The standard deviations between the measurements, biases of the radar estimates from the S4 measurements and correlation coefficients are given in Table I.

Differences in results from the two instruments may be partly due to the fact that the SeaSonde gives an area measurement and the S4 current gives a point measurement closer to shore (see Fig. 2).

Fig. 7 shows the wind direction calculated using the methods described in Section V-B.

During the period there were several storms, and the ocean wave spectrum contained both long-period swell and wind-wave components. Swell and wind sea usually have different periods

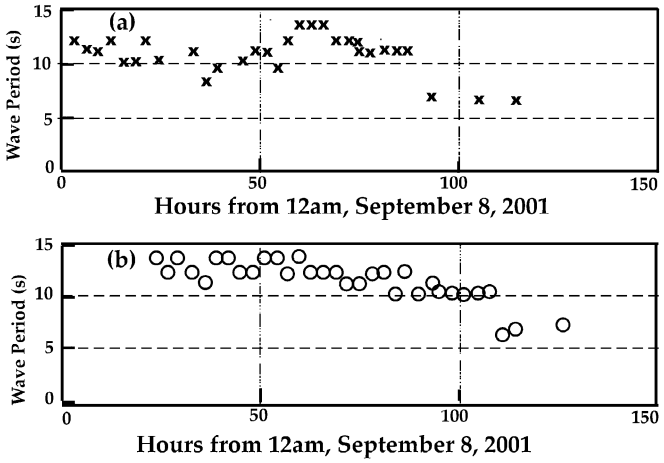

Fig. 10. Wave periods measured with long-range SeaSondes located at Hachijo and Nojima during a storm, September 2001. (a) Hachijo. (b) Nojima.

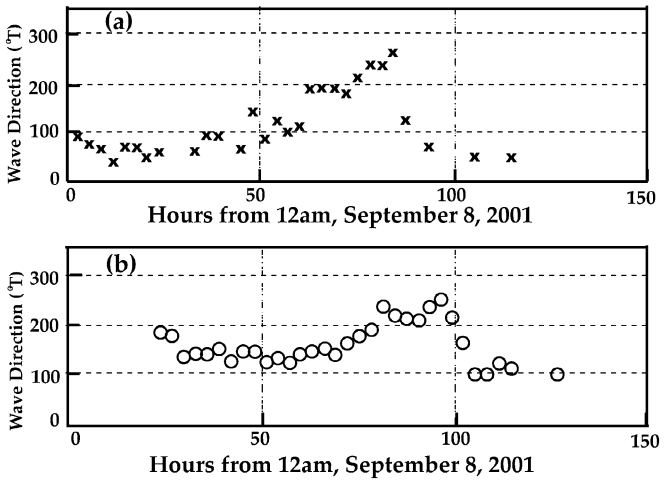

Fig. 11. Wave directions measured with long-range SeaSondes located at Hachijo and Nojima during a storm, September 2001. For Nojima, located on the coast, the analysis assumes that waves of period greater than 6 s are onshore, as discussed in Section IV-A. For Hachijo, located on an island, the analysis places no restriction on wave direction. (a) Hachijo. (b) Nojima.

and directions. The ocean wave spectrum defined by (9) and (10) contains only a single component, derived results for wave period and direction depend on whether swell or wind waves is selected as the dominant component. In future work, we plan to employ a model that includes both swell and wind-wave components.

B. Japan Coast Guard Hydrographic Department

As a second example, we used a data set taken by two long-range SeaSondes at Hachijo Island and Nojima on the mainland; see Fig. 8 for the locations. Here, the second range cell was chosen for analysis. The water depth well exceeded that needed for our analysis. Wave information was obtained using model-fitting.

As is typical with long-range systems, the low-energy second-order structure emerges from the noise floor only for high waves. Figs. 9–12 show the wave height, period, direction, and the wind direction measured during a typhoon in September 2001.

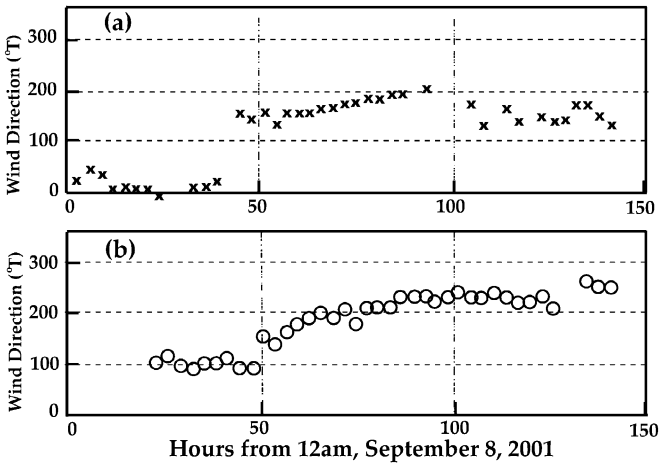

Fig. 12. Wind directions measured with long-range SeaSondes located at Hachijo and Nojima during a storm on September, 2001. (a) Hachijo. (b) Nojima.

C. Oregon State University

As a third example, we used a data set taken by SeaSondes throughout a severe winter storm on the Oregon coast: a long-range unit at Winchester Bay and a standard-range unit at Washburn: see Fig. 13 for the locations. Wave information was obtained from model fitting. Results for waveheight, centroid period, direction and wind direction for both standard and long-range units are shown in Figs. 14 and 15. This data set illustrates the complementary nature of long-range and standard-range systems. Before the height of the storm and after the waves have died down, information is provided by the standard-range system. But for the period of the highest waves, when the standard-range radar spectra are saturated, the information is provided by the long-range system.

VIII. Conclusion

We have described techniques for the derivation of wave directional information from Seasonde data. Integral inversion can be used with standard-range SeaSondes to provide the ocean wave spectrum from high-quality, low-noise radar spectra, when the waveheight is below the saturation limit. Model fitting can be applied under a wide range of conditions and is used by our operational software to give estimates of waveheight, centroid period and direction for both standard-range and long-range SeaSondes.

We have discussed the tradeoffs in the choice of radar transmit frequency for wave observations. On one hand, the radar frequency needs to be sufficiently high for the second-order energy to emerge from the noise floor. On the other hand, the saturation limit on waveheight for the production of wave information is inversely proportional to the radar frequency. We recommend implementing a new low-power HF radar instrument, designed exclusively for wave measurement, with the capability of switching transmit frequency from 13 to 5 MHz as the waveheight approaches the saturation limit. As wave information is derived from close-in radar range cells, system power requirements for wave measurement are low, reducing the projected hardware cost. Operating in the 13-MHz band, this instrument would give wave information for low and

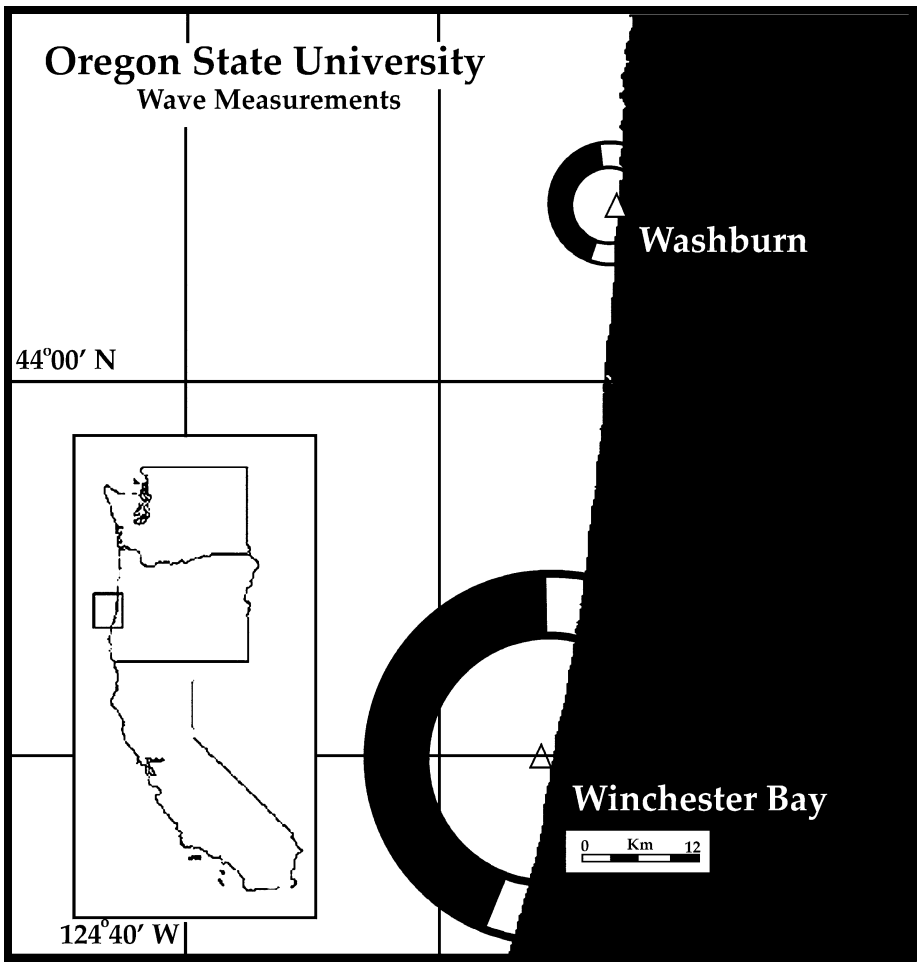

Fig. 13. The locations of the long-range SeaSonde at Winchester Bay and the standard-range SeaSonde at Washburn. The inset map shows the location on the Oregon coast. Radar sea-echo from the second range cell is analyzed to give wave information. Radar coverage in the range cell is restricted by obstructing land to the shaded area shown.

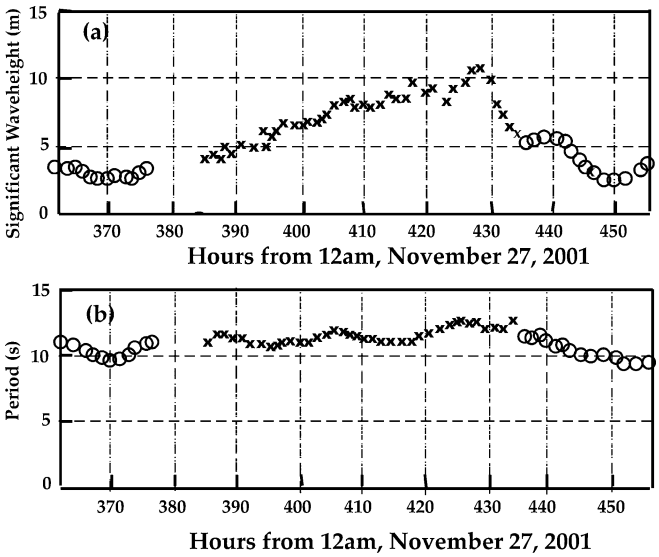

Fig. 14. (a). Significant waveheight measured with a long-range SeaSonde located at Winchester Bay, Oregon (crosses) and a standard-range SeaSonde at Washburn, Oregon (circles). (b). Wave periods measured with a long-range SeaSonde located at Winchester Bay, Oregon (crosses) and a standard-range SeaSonde at Washburn, Oregon (circles).

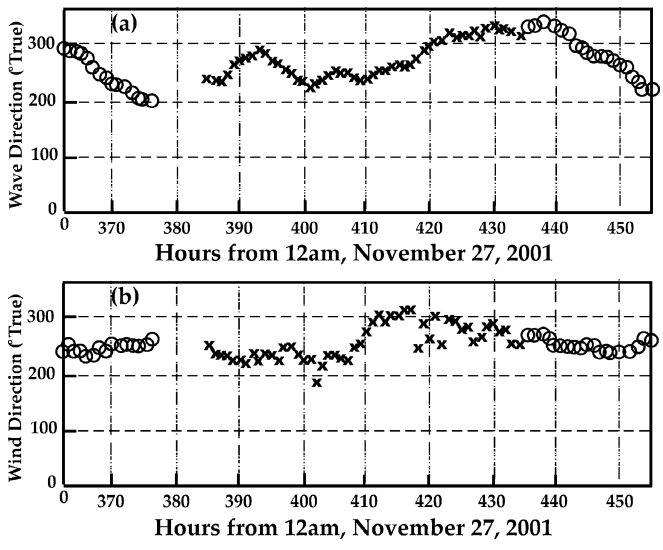

Fig. 15. (a). Wave directions measured with a long-range SeaSonde located at Winchester Bay, Oregon (crosses) and a standard-range SeaSonde at Washburn, Oregon (circles). The analysis assumes that waves of period greater than 6 s are onshore, as discussed in Section IV-A. (b). Wind directions measured with a long-range SeaSonde located at Winchester Bay, Oregon (crosses) and a standard-range SeaSonde at Washburn, Oregon (circles).

moderate waveheights. If the waveheight increases toward the 13-MHz saturation limit, the transmit frequency would switch to 5 MHz, when the waveheight would be well below the saturation limit. Alternatively, the frequency could alternate 5 and 13 MHz, providing continual coverage. Such a system would be able to measure waves under virtually all waveheight conditions.

ACKNOWLEDGMENT

The authors thank the following people and organizations for providing access to the SeaSonde data described in this paper. The Environmental and Oceanographic Research Division of the Hydrographic and Oceanographic Department, Japan Coast Guard; Dr. M. Kosro, Oregon State University; and Dr. J. Paduan, Naval Postgraduate School, Monterey, CA.

REFERENCES

[1] D. D. Crombie, "Doppler spectrum of sea echo at 13.56 MHz," *Nature*, vol. 75, pp. 681–682, 1955.

[2] D. E. Barrick, "First-order theory and analysis of MF/HF/VHF scatter from the sea," *IEEE Trans. Antennas Propag.*, vol. AP-20, pp. 2–10, 1972.

[3] ——, "Remote sensing of sea-state by radar," in *Remote Sensing of the Troposphere*, V. E. Derr, Ed., 1972, pp. 12-1–12-46.

[4] L. R. Wyatt, "Ocean wave parameter measurements using a dual-radar system, a simulation study," *Int. J. Remote Sensing*, vol. 8, pp. 881–891, 1987.

[5] ——, "Significant waveheight measurement with HF radar," *Int. J. Remote Sensing*, vol. 9, pp. 1087–1095, 1988.

[6] ——, "A relaxation method for integral inversion applied to HF radar measurement of the ocean wave directional spectrum," *Intl. J. Remote Sensing*, vol. 11, pp. 1481–1494, 1990.

[7] ——, "High order nonlinearities in HF radar backscattering from the ocean surface," *IEEE Proc. Radar, Sonar Navig.*, vol. 142, pp. 293–300, 1990.

[8] L. R. Wyatt and L. J. Ledgard, "OSCR wave measurements—Some preliminary results," *IEEE J. Ocean. Eng.*, vol. 21, pp. 64–76, 1996.

[9] R. Howell and J. Walsh, "Measurement of ocean wave spectra using narrow-beam HF radar," *IEEE J. Ocean. Eng.*, vol. OE-18, pp. 296–305, 1993.

[10] Y. Hisaki, "Nonlinear inversion of the integral equation to estimate ocean wave spectra from HF radar," *Radio Sci.*, vol. 31, pp. 25–39, 1996.

[11] N. Hashimoto, L. R. Wyatt, and S. Kojima, "Verification of a Bayesian method for estimating directional spectra from HF radar surface backscatter," *Coastal Eng. J.*, vol. 45, pp. 255–274, 2003.

[12] B. J. Lipa and D. E. Barrick, "Analysis methods for narrow-beam high-frequency radar sea echo,", NOAA Tech. Rep. ERL 420-WP, vol. 56, 1982.

[13] Y. Hisaki, "Correction of amplitudes of Bragg lines in the sea echo doppler spectrum of an ocean radar," *J. Atmos. Ocean. Technol.*, vol. 16, pp. 1416–1433, 1999.

[14] B. J. Lipa and D. E. Barrick, "Extraction of sea state from HF radar sea echo: Mathematical theory and modeling," *Radio Sci.*, vol. 21, pp. 81–100.

[15] ——, "Least-squares methods for the extraction of surface currents from CODAR crossed-loop data: Application at ARSLOE," *IEEE J. Ocean. Eng.*, vol. OE-8, pp. 226–253, 1983.

Belinda Lipa received the Ph.D. degree in theoretical physics from the University of Western Australia.

She was a research associate with Stanford University, CA, from 1974 to 1978, working on the interpretation of narrow-beam HF radar sea-echo to give parameters of the directional ocean wave spectrum, and continued this work at SRI International. In 1980, she formed a private company with the purpose of developing software to give ocean surface information from sea-echo received by small broad-beam HF radar systems. Since 1986, she has been vice president of Codar Ocean Sensors, a small company that develops and markets the SeaSonde, a compact radar for the measurement of ocean surface current maps and directional wave spectra in coastal waters.

Bruce Nyden received the Master's degree in geography (remote sensing) from San Diego State University, CA.

He was a research technician with San Diego State University from 1991 to 2000 and worked on change detection of coastal salt marsh vegetation using low altitude multispectral imagery. He joined the Bodega Marine Laboratory, University of California, Davis, in 2000 where he was a Geographic Information System and Marine Instrumentation specialist. In 2002, he joined Codar Ocean Sensors, and currently manages the Customer Support Group.